Letter
Chinese Science Bulletin
Condensed Matter Physics
February 2012 Vol.57 No.6: 565–568
doi: 10.1007/s11434-011-4920-2

Anisotropic Raman spectroscopy of a single β-Ga_2O_3 nanobelt

SUN Zheng, YANG LinHong, SHEN XueChu & CHEN ZhangHai*

State Key Laboratory of Surface Physics and Department of Physics, Laboratory for Advanced Materials, Fudan University, Shanghai 200433, China

Received October 5, 2011; accepted November 14, 2011

The polarization dependence of the Raman spectra of a single ultra-wide β-Ga_2O_3 nanobelt was studied. The spectra were found to strongly depend on the relative angle between the polarization of the incident light and the axis of the β-Ga_2O_3 nanobelt. Such behavior was ascribed to the large length to width ratio of the nanostructure and its small dielectric constant. The ultra-wide β-Ga_2O_3 nanobelt was fabricated using catalyst-free thermal chemical vapor deposition.

Raman spectroscopy, gallium oxide, polarization, nanostructure

Citation: Sun Z, Yang L H, Shen X C, et al. Anisotropic Raman spectroscopy of a single β-Ga_2O_3 nanobelt. Chin Sci Bull, 2012, 57: 565–568, doi: 10.1007/s11434-011-4920-2

Monoclinic gallium oxide (β-Ga_2O_3) is a promising wide-band-gap semiconductor (E_g=4.9 eV at 300 K) having good chemical and thermal stability. It can be used in a wide range of applications, such as semiconducting lasers, as a transparent conducting oxide, and in switching memories and high temperature gas sensors [1–5]. In the past few years, attention has been paid to synthesizing nanoscale β-Ga_2O_3 because of its potential in device applications [3]. Various fabrication methods have been developed such as laser ablation [6], carbothermal reduction [7,8], arc discharge [9], thermal evaporation [10], and chemical vapor deposition [11,12]. Among the nanoscale structures of β-Ga_2O_3 nanosheets, nanobelts are important for the unique optical and electrical properties, which result from their quasi-two-dimensional (quasi-2-D) structure. Besides the possible quantum confinement effects on the electrical states, optical anisotropies due to the structural anisotropies are expected.

Although Raman spectroscopy has been used by several research groups to study β-Ga_2O_3 [13,14], little attention has been paid to the polarization dependence of the Raman scattering of a single β-Ga_2O_3 nanobelt, although it may reveal the anisotropic properties of the crystalline structures. Indeed, when the β-Ga_2O_3 transforms from the bulk to a 2-D nanobelt, the effective electric field inside the sample changes its orientation and thus induces polarization dependence of the Raman spectra of the sample.

In this work, we report a catalyst-free and large-scale synthesis of ultra-wide β-Ga_2O_3 nanobelts by thermal chemical vapor deposition using pure bulk Ga (99.99999%). Raman scattering measurements were carried out on a single ultra-long β-Ga_2O_3 nanobelt. We find that the Raman spectra depend strongly on the relative angle between the polarization of the incident light and the long axis of the β-Ga_2O_3 nanobelt. This behavior is ascribed to the large ratio of length to width and the small dielectric constant of the β-Ga_2O_3 nanobelt.

Ultra-long β-Ga_2O_3 nanobelts were synthesized by thermal chemical vapor deposition without using a catalyst [15,16]. The typical process is as follows: a clean silicon wafer substrate was dried in a drying cabinet for 15 min. Gallium metal (99.99999%) was cut into small pieces and loaded onto a quartz boat while the Si was placed at the downstream end of the boat, 10 mm away from the Ga source. The quartz boat was placed in the center of a long ceramic tube and the boat and tube were inserted into a hor-

*Corresponding author (email: zhanghai@fudan.edu.cn)

izontal furnace. Then the furnace was heated to 950°C, and maintained at this temperature for 2 h in a flow of N_2 (flow rate 2 sscm). Then the furnace was cooled naturally. After cooling down to room temperature, we obtained a white wool-like product. The morphology and microstructure of the samples were characterized using X-ray diffraction (XRD, Bruker D8 ADVANCE and DAVINCI.DESIGN), field emission scanning electron microscopy (SEM, Hitachi S-4800) and transmission electron microscopy (TEM, JEOL JEM-2100F). Raman scattering measurements were carried out with a confocal micro-Raman spectrometer (HORIBA-Jobin Yvon LabRam HR 800UV). We selected a single β-Ga_2O_3 nanobelt with its long axis (the axis parallel to the long side of the rectangular sample) for the Raman measurement. All the Raman spectra were measured in backscattering geometry using a He-Ne laser (632.8 nm) as the excitation source.

Figure 1(a) illustrates the XRD of the as synthesized β-Ga_2O_3 nanobelts. The nanobelts and the bulk polycrystalline β-Ga_2O_3 have the same diffraction peaks, which are indexed as the monoclinic structure (a=12.23 Å, b=3.04 Å, c=5.8 Å). The lattice constants of the crystal are in good agreement with previous observations [1,2,7,17]. It should be noted that the strongest peak of the XRD signal is (400) instead of (111). This is common in nano-sized structures and can be explained by the size-effect and disorder arising in the nanostructures [15]. Figure 1(b) shows the SEM image of the as synthesized β-Ga_2O_3 nanobelts. The sheets are several micrometers wide, while the length of the nanobelt is hundreds of micrometers. The thickness of the sheets, in contrast to the width and the length, is only dozens of nanometers. One can see from Figure 1(c) that the nanobelts are intact slices peeled from the Ga ingot and the shape of the belts is rectangular. Figure 2(a) shows the low magnification TEM image of the β-Ga_2O_3 nanobelts. The waving

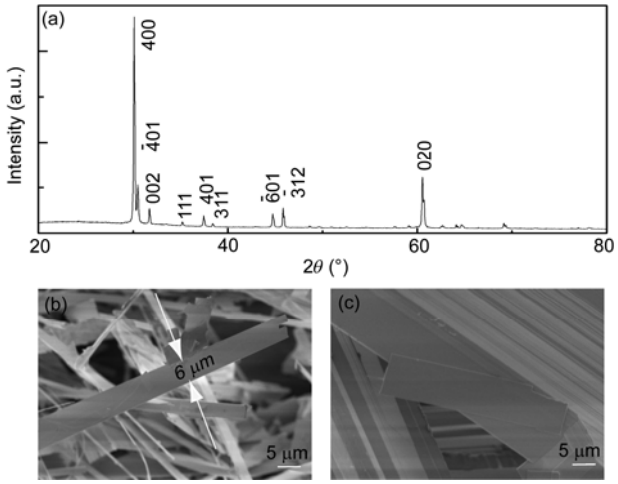

Figure 1 (a) XRD pattern obtained from the β-Ga_2O_3 nanobelts. (b), (c) SEM images of the as-synthesized β-Ga_2O_3 nanobelts formed from pure Ga powder at 950°C.

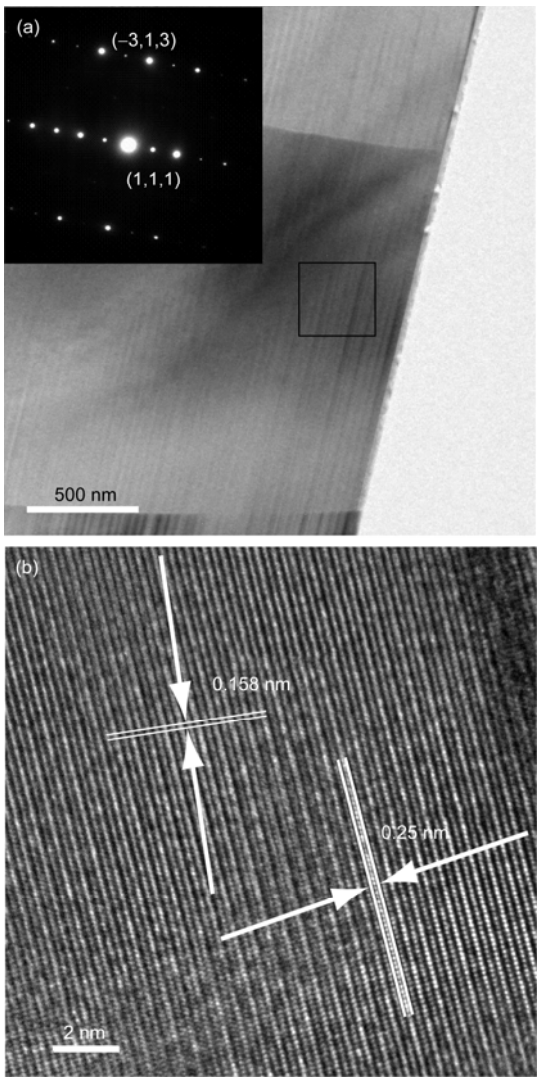

Figure 2 (a) Low magnification TEM image of the β-Ga_2O_3 nanobelts (the inset is the corresponding electron diffraction pattern); (b) high resolution TEM image of the area in the square in (a).

shapes can be seen clearly. The contrast observed on the nanobelts results from bending of the nanobelts as they interact with the electron beam. This is a typical electron diffraction phenomenon that can be observed in metal foils because of bending or deformation [18]. Figure 2(b) shows the high resolution TEM image of a single nanobelt. It can be concluded from the image that the sample we fabricated is a single-crystal structure with negligible defects. The inset in Figure 2(a) is the selected area electron diffraction (SAED) pattern.

It is known that β-Ga_2O_3 is a monoclinic structure with space group symmetry C_{2h} [13]. Group theory analysis predicts the following acoustical and optical center modes: $\Gamma_{aco}=A_u+2B_u$ and $\Gamma_{aco}=10A_g+4A_u+5B_g+8B_u$ [14] (The optical modes A_g and B_g are Raman active, and the other two optical modes A_u and B_u are infrared active). Figure 3 shows the Raman spectra of bulk Ga_2O_3 and our nanobelt

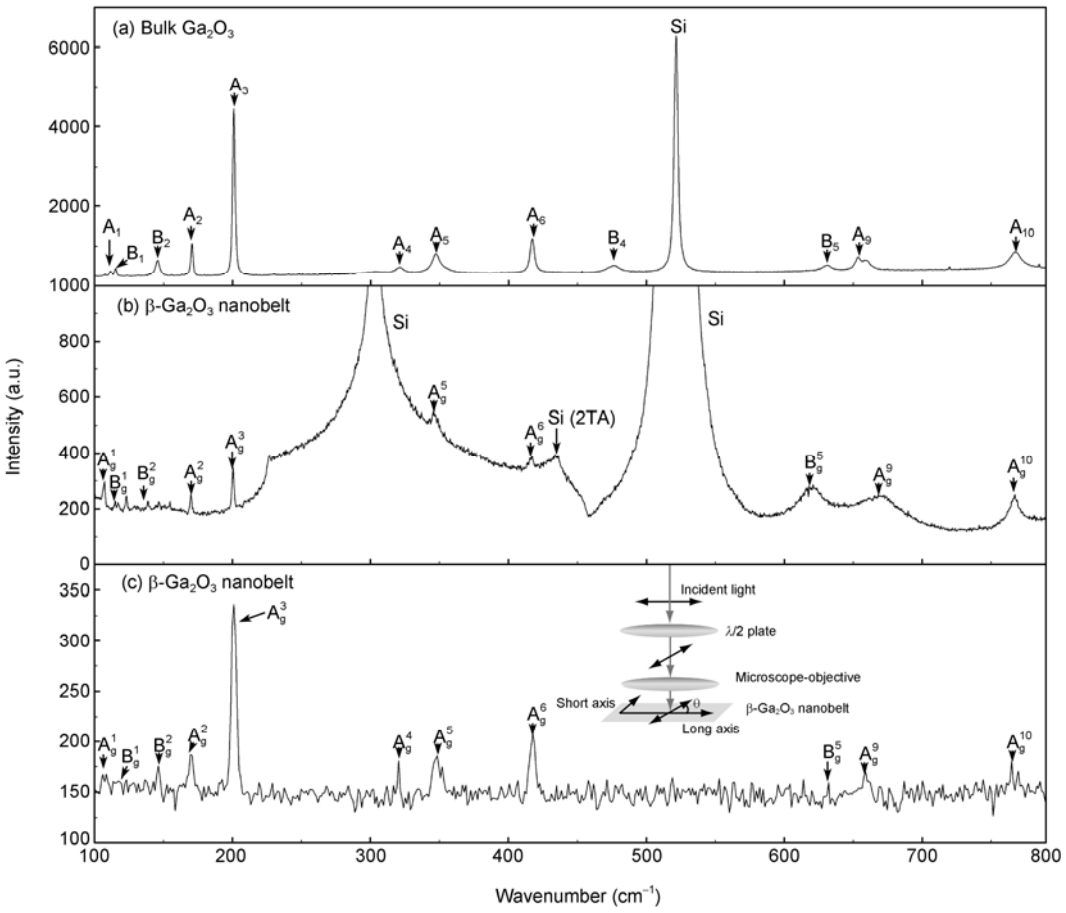

Figure 3 (a) Unpolarized Raman spectrum of bulk Ga_2O_3. (b) Unpolarized Raman spectrum of a single β-Ga_2O_3 nanobelt which is set on the Si wafer. The A_4 mode cannot be resolved because of the strong intensity of the Si peak. (c) Unpolarized Raman spectrum of a single β-Ga_2O_3 nanobelt which is set on glass. The A_4 mode appears again, while the Si (2TA) mode disappears. The inset diagram shows the geometry of the Raman measurement.

sample, excited by a 632.8 nm He-Ne laser. It can be seen from the figure that not all the optical modes can be detected, which is in good agreement with the results that have been reported by Dohy et al. [19]. It is possible that the "missing" Raman modes are suppressed by the stronger adjacent Si peaks or the other Raman peaks. Therefore, the β-Ga_2O_3 nanobelts were set on glass and measured again. We found that the A_4 mode, which cannot be resolved in Figure 3(b), appears in Figure 3(c) because the strong intensity of the Si peak has gone. All the Raman spectra were measured under the backscattering geometry. The modes B_g^5 and A_g^9 of β-Ga_2O_3 nanobelts in Figure 3(b) are broader than those from the bulk sample and they shifted a little with respect to those of the commercial bulk Ga_2O_3. However, the modes B_g^5 and A_g^9 of β-Ga_2O_3 nanobelts in Figure 3(c) are similar to the same modes in Figure 3(a). It is obvious that some spectral features in the Raman spectrum of the β-Ga_2O_3 nanobelt sample are related to the Si wafer, such as the peaks at 300, 435, 620 and 670 cm^{-1}, which result from the two-phonon 2TA(L), 2TA(Σ) scattering, and a combination of optical and acoustic phonons in the Σ direction, respectively [20].

In our experiment, the angle between the short axis along the short side of the rectangular sample and the polarization direction of the incident light is tuned from 0° to 360° using a half-wave plate as shown in the inset diagram of Figure 3. Seven peaks (106, 168, 200, 347, 416, 658 and 767 cm^{-1}) are detected. They correspond to the A_g modes of the β-Ga_2O_3 nanobelt [14]. One can see that all the observed A_g modes show polarization dependence, demonstrating an obvious oscillation of intensity as a function of the angle. However, in contrast, the B_g modes do not show this type of behavior.

We fitted the intensity of all the A_g modes with

$$I(\theta) = I(0^\circ)\cdot\left(1-\frac{1-\rho}{1+\rho}\sin^2\theta\right), \quad (1)$$

where θ is the angle between the polarization of the incident light and the short axis of our sample and ρ is the depolarization ratio of the Raman band [21], as shown in Figure 4. The intensity of the Raman peaks oscillates with a period of 180°. Most interestingly, all the intensities of A_g modes are

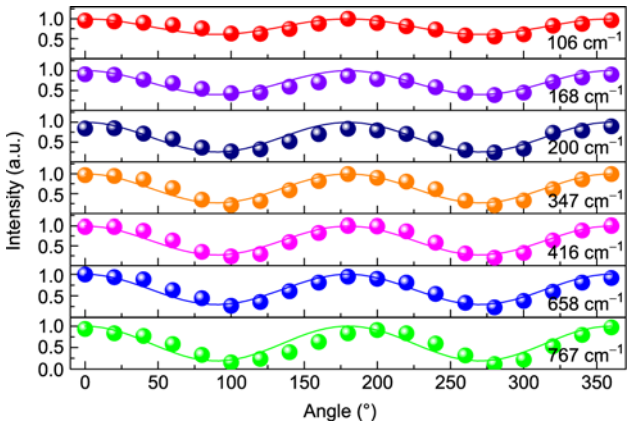

Figure 4 The relative intensity of the 7 Raman modes as a function of the angle θ, between the short axis of a single β-Ga_2O_3 nanobelt and the polarization direction of the incident laser. The solid spheres are experimental data, and the solid curves are fitted by using eq. (1). Note that all the strongest intensity peaks are at θ=0°, 180°, 360°, while the weakest intensity peaks are at θ=90°, 270°.

strongest when the polarization direction of the incident light is perpendicular to the long axis of our sample (θ=0°, 180°, or 360°) and the weakest when they are parallel (θ=90° and 270°). This can be explained by the classical theory of electric fields in dielectrics. The electric field of the incident laser polarized perpendicular to the long axis of the nanobelts is modulated because of the width scale compared to the wavelength. This can be described as

$$E_i = \frac{2\varepsilon_0}{\varepsilon + \varepsilon_0} E_e, \quad (2)$$

where E_i is the electric field in the nanobelts, E_e is the excitation field, $\varepsilon(\varepsilon_0)$ is the dielectric constant of gallium oxide (vacuum) [22]. On the other hand, the polarized electric field parallel to the long axis of the nanobelts could be considered to be the same as that in the bulk and can be described as

$$E_i = \frac{1}{\varepsilon} E_e. \quad (3)$$

Since $\varepsilon_{Ga_2O_3}$=1.8−1.9 [14], this indicates that the intensity perpendicular to the long axis is relatively larger than that along the long axis and the peak intensity reveals $\sin^2\theta$ dependence. The result we obtain from the thoery agrees quite well with our experimental data. The large ratio of length to width is responsible for the novel intensity oscillation.

In summary, single β-Ga_2O_3 nanobelts were synthesized by a simple chemical vapor deposition method. XRD and TEM analysis revealed that our samples are pure β-Ga_2O_3 and have good crystallinity. Furthermore, the polarized Raman scattering spectra were measured for a single β-Ga_2O_3 nanobelt. The intensity is polarization dependent, with an oscillation period of π. We fitted it with equations from classical electric field theory and found the analysis agrees well with our experimental results. The polarization dependence of the Raman modes can be attributed to the modulation of the electric field inside the nanobelt, which is due to the large ratio of length to width.

This work was supported by the National Natural Science Foundation of China and the National Basic Research Program of China (2011CB925602, 2010DAF0260).

1 Xiang X, Cao C B, Zhu H S. J Cryst Growth, 2005, 279: 122–128
2 Chun H J, Choi Y S, Bae S Y, et al. J Phys Chem B, 2003, 107: 9042–9046
3 Liang C H, Meng G W, Wang G Z, et al. Appl Phys Lett, 2001, 78: 3202–3204
4 Ho H P, Lo K C, Fu K Y, et al. Chem Phys Lett, 2003, 382: 573–577
5 Choi Y C, Kim W S, Park Y S, et al. Adv Mater, 2000, 12: 746–750
6 Hu J Q, Li Q, Meng X M, et al. J Phys Chem B, 2002, 106: 9536–9540
7 Wu X C, Song W H, Huang W D, et al. Chem Phys Lett, 2000, 328: 5–9
8 Li Z J, Li H J, Chen X L, et al. J Alloys Compd, 2002, 345: 275–279
9 Park G S, Choi W B, Kim J M, et al. J Cryst Growth, 2000, 220: 494–500
10 Kim N H, Kim H W. Appl Surf Sci, 2005, 242: 29–34
11 Kim N H, Kim H W, Seoul C, et al. Mater Sci Eng B, 2004, 111: 131–134
12 Kim H W, Kim N H. Appl Surf Sci, 2004, 233: 294–298
13 Rao R, Rao A M, Xu B, et al. J Appl Phys, 2005, 98: 094312
14 Liu B, Gu M, Liu X L. Appl Phys Lett, 2007, 91: 172102
15 Zhang H Z, Kong Y C, Wang Y Z, et al. Soild State Commun, 1999, 109: 677–682
16 Pan Z W, Dai Z R, Wang Z L. Science, 2001, 291: 1947–1949
17 Khan A, Jadwisienczak W M, Kordesch M E. Physica E, 2006, 35: 207–211
18 Hirsch P B, Howie A, Nicholson R B, et al. Electron Microscopy of Thin Crystals. Oxford: Butterworth Heinmann, 1965
19 Dohy D, Lucazeau G, Revcolecschi A. J Solid State Chem, 1982, 45: 180–192
20 Tan P H, Brunner K, Bougeard D, et al. Phys Rev B, 2003, 68: 125302
21 Leipertz A, Fiebig M. Appl Opt, 1980, 19: 2272–2274
22 Landu L D, Lifshitz E M, Pitaevskii L P. Electrodynamics of Continuous Media. Oxford: Pergamon, 1984